

# APPARENT PULSE DIFFUSION DUE TO DISORDERED MICROSTRUCTURE

A. Nachbin\* and K. Sølna†

\*Instituto de Matemática Pura e Aplicada  
Est. D. Castorina 110, Jardim Botânico  
Rio de Janeiro, RJ 22460-320, Brazil  
e-mail: nachbin@impa.br

<http://www.impa.br/Pesquisadores/AndreNachbin>

†Department of Mathematics, University of Utah  
Salt Lake City, Utah, 84112, USA  
e-mail: solna@math.utah.edu

**Key words:** random media, acoustic waves, water waves.

**Abstract:** Wave propagation in disordered (random) media is the underlying theme. Many types of wave propagation problems can most conveniently be analyzed in this framework. Acoustic waves in the earth's crust and shallow water (or surface gravity) waves are two examples. The interaction of sound waves with the heterogeneities in the earth's crust is important in seismology. The interaction of surface gravity waves with rough submerged obstructions has been analyzed extensively because of its importance in oceanography. It is also important in the development of new techniques for analyzing scattering problems in fluid mechanics.

The theory to be outlined in this paper had its first application in seismic exploration. The earth is strongly heterogeneous, also on small scales, and it is important to describe when and how fine scale heterogeneities interact with a traveling seismic pulse.

We are interested in pulse shaped waves that interact with the rapidly varying features (i.e. microstructure) of the medium. The multiple scattering associated with the disordered microstructure, leads to the apparent diffusion of the propagating pulse. That is, the pulse diffuses about its moving center due to the multiple scattering of the wave energy.

We present a summary of the asymptotic theory that describes the interaction of a propagating pulse with the medium's microstructure. Also we describe the connection between acoustic and shallow water pulse shaping or apparent diffusion. We consider media having general smooth background variations, with a locally laminated disordered microstructure. Theoretical results are validated through numerical experiments. Acoustic wave experiments are performed in a Goupillaud medium. In the context of water waves the numerical model consists of a semi-implicit, semi-Lagrangian discretization of the hydrostatic Navier-Stokes equation in three dimensions. We show that the numerical experiments capture very well different types of behavior predicted by the theory.

# 1 Introduction

## 1.1 Motivation

Our objective is to discuss wave propagation in disordered or random media. That is, we consider a wave pulse that propagates through a medium whose parameters vary randomly. The main result we present in this paper is that the random medium fluctuations cause the propagating pulse to broaden as it travels. Due to multiple scattered energy, the pulse appears to diffuse about a moving center. The amount of broadening, or apparent diffusion, of the wave pulse is proportional to the square root of the traveling distance. Moreover, the *apparent diffusion* depends only on the traveling distance and the *statistics* of the random medium fluctuations. Thus, the broadening can be described in a deterministic way independently of the particular medium realization. However, as we show below, the *velocity* of the wave pulse contains a small *random* component. In the sequel we refer to the transformation of the pulse due to the microscale medium fluctuations as *pulse shaping*.

In the effective medium approximation the random medium fluctuations are replaced by a deterministic *effective medium*. This approximation is only valid for relatively short propagation distances, on the order of a few pulse lengths. Wave propagation in the effective medium is non-diffusive and does not capture the broadening of the pulse that becomes important for *long* propagation distances.

The theory for pulse shaping was derived in the context of acoustic wave propagation in the earth's crust. We motivate the random medium model in terms of this application, but also point out to other applications where the theory plays a role. We shall consider a model medium that we define as a *locally layered random medium*. The locally layered random medium has general, three dimensional, deterministic background variations with a randomly locally laminated microstructure. The model is motivated by sedimentary rock structures where sedimentary cycles produce a tilted stack of layers. On top of this local variation there are coarse scale features that come from macroscopic geological events. For such a medium we have analyzed [19, 21] the spreading of an acoustic pulse due to the microscale variations in the medium parameters and in Section 5 we summarize the results.

The motivation for modeling in terms of a random medium is that a detailed description of the effects of the rough microscale medium fluctuations are often not possible. Moreover, the details of this fluctuations are typically not known. However, if we model in terms of a random medium with known, perhaps slowly varying, statistics the accumulated effect of the disordered or random component of the medium, can in many cases, be characterized. With this approach, uncertainties about a specific medium are translated into uncertainties about a transmitted pulse shape in a systematic way. Moreover, typical pulse shaping can be examined and characterized. For the problem at hand the broadening of the pulse traveling through the earth's crust can actually be described in a deterministic way, to leading order, assuming that the statistics of the random variations in the earth's parameters are known.

## 1.2 Related work

If the medium is purely one-dimensional, or layered, the pulse shaping problem has been studied extensively. In this case the behavior of the front of the pulse, over long distances, can be analyzed using asymptotic results for stochastic ordinary differential equations [11]. The study of the effect of fine scale layering on a propagating pulse was initiated by O’Doherty and Anstey [18]. They give a quantitative explanation of the pulse shaping in terms of the statistics of the reflection coefficients for a Goupillaud medium, that is, a discretely layered medium in which the travel or transit time of each layer is constant. Their motivation for studying pulse spreading was to explore whether scattering associated with fine scale layering in the earth could explain the observed damping of seismic waves. In a series of papers [1, 2, 3, 4, 5, 7, 12, 13, 20] the O’Doherty-Anstey approximation and its generalizations have been rigorously derived, under various conditions for the medium model. They all assume, however, a strictly layered medium.

In [19, 21] and this paper we follow the line of research initiated by O’Doherty and Anstey, but consider more general three-dimensional wave propagation problems.

## 1.3 Outline of paper

In Section 2 we describe the model for the locally layered medium and the important scaling assumptions concerning pulse width and magnitude of the medium fluctuations. To fix ideas about pulse shaping we give a numerical example in Section 3. This example concerns a model with a purely layered medium. In the absence of the microscale random medium fluctuations the pulse propagation can be described in the geometrical optics or high frequency approximation. In Section 4 we give a brief account for this approximation. The main result characterizing pulse shaping in the locally layered random medium can be seen as a combination of the geometrical optics approximation with pulse shaping theory for a layered medium. We show this in Section 5 where we present the general pulse shaping approximation. Finally, in Section 6 we discuss the pulse shaping approximation in the context of shallow water waves propagating over a rough bottom and present 3D numerical experiments.

## 2 Model

We consider acoustic pulse propagation in three space dimensions. A basic feature of the medium model is that it varies on two scales: a macroscale corresponding to the total travel distance and a microscale corresponding to that of the random fluctuations. The width of the probing pulse is taken to be large relative to the microscale but small relative to the macroscale. This scaling is relevant for seismic exploration where the pulse width is chosen so that it can resolve large scale features. In the seismic exploration context the total travel distance might be about  $10km$ , the width of the pulse  $100m$  and the scale of the inhomogeneities  $1m$ .

Following [21] let  $\mathbf{u}(\mathbf{x}, z, t)$  and  $p(\mathbf{x}, z, t)$  be the acoustic velocity and pressure solving

the equations of conservation of momentum and mass

$$\rho \mathbf{u}_t + \nabla p = f(t/\varepsilon)\delta(\mathbf{x})\delta(z - z_s)\mathbf{e} \quad (1)$$

$$K_\varepsilon^{-1}(\mathbf{x}, z) p_t + \nabla \cdot \mathbf{u} = 0.$$

Here  $t$  is time,  $z$  is depth into the medium and  $\mathbf{x} = (x_1, x_2)$  are the horizontal coordinates.

The parameters  $\rho$  and  $K_\varepsilon^{-1}$  are the density and compliance,  $f$  is the pulse shape and  $\mathbf{e} = (e_1, e_2, e_3)$  is a source directivity vector. We let the source be located at  $(0, 0, z_s)$ , with  $z_s < 0$ , and choose the halfspace  $z < 0$  to be homogeneous. The parameter  $\varepsilon$  is the ratio of the pulse width to the travel distance and is assumed small. The pulse width  $\varepsilon$  is intermediate between the size of the fluctuations  $\varepsilon^2$  and the travel distance which is of order 1. The density and compliance have the form

$$\rho(\mathbf{x}, z) \equiv \rho_0 \quad (2)$$

$$K_\varepsilon^{-1}(\mathbf{x}, z) = \begin{cases} K_0^{-1} & z < 0 \\ K_1^{-1}(\mathbf{x}, z)(1 + \nu(z)/\varepsilon^2) & z > 0 \end{cases}.$$

The random modulation  $\nu(\cdot)$  of the compliance is stationary with mean zero and finite, decaying correlation function. In the general case  $\nu$  can be made to depend on a set of smooth level curves  $\phi : \nu = \nu(\phi(\mathbf{x}, z)/\varepsilon^2)$ , see [19]. We refer to this medium as a **locally layered** random medium. We are interested in the form of the transmitted pulse in such a medium when  $p$  and  $\mathbf{u}$  are zero initially.

The above scaling is not the only scaling of interest. In [19] we also analyze the case where the medium fluctuations are *weak*, order  $\varepsilon$ , and the probing pulse is supported on the scale of the medium fluctuations, the scale  $\varepsilon^2$ . We are able to derive similar results with this scaling as for the one discussed above.

The model is relevant in other applications as well. In Section 6 we point to its significance in analyzing shallow water waves propagating over a rough bottom. We also point out that disturbances propagating through mechanical structures are affected by local variations of the medium parameters. The above model for wave-propagation is relevant for instance in nondestructive testing of ‘wave’-fiber composites or laminates, [9, 10]. We have presented the model in the context of sound propagation through the earth’s crust, but it is relevant also for sound propagation through the ocean, [8].

### 3 Illustration of pulse shaping

In this section we give an example of pulse shaping for acoustic wave propagation in a one-dimensional or purely layered medium. The medium is discretized into a Goupillaud medium. Thus, the medium comprises a stack of layers where the transit time of each

layer is constant, but the impedance in the different layers fluctuate randomly. The

impedance is  $\xi = \sqrt{K_\varepsilon \rho_0}$ . For simplicity we assume that the impedances in the different layers are independent. The relative fluctuations are 10 % and normally distributed. For a Goupillaud medium the pulse propagation can be simulated in a particularly efficient way since only the pulse front need to be explicitly represented. On entering the stack of layers the pulse is a Dirac delta function.

In Figure 1 we show transmitted pulse shapes after propagation through the discrete medium. The 20 dotted lines correspond to propagation through different realizations of the medium. The transmitted pulses are plotted at a *fixed depth* and relative to the arrival of the ‘leading’ pulse. The average number of medium layers for the chosen depth is 10,000. Note that the travel time to the fixed depth (which depends on the realization) is random. However, it can be shown that the average travel time for the pulses coincides with the effective medium travel time.

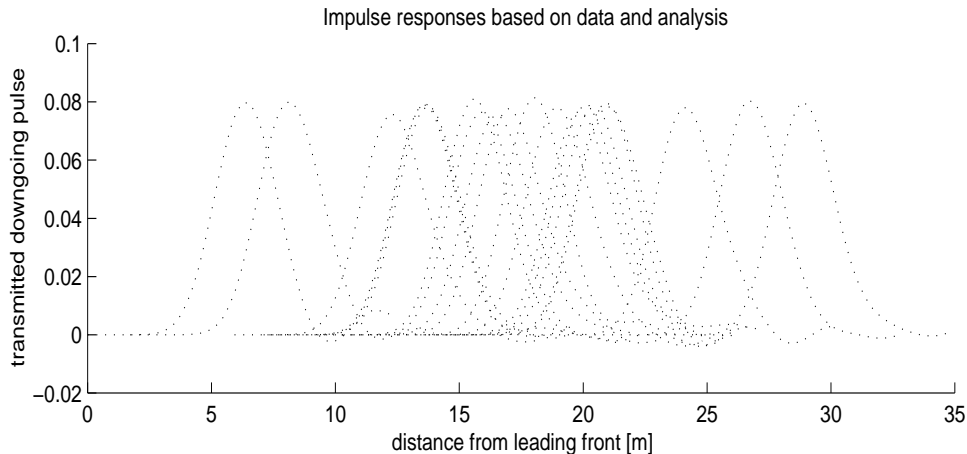


Figure 1: The transmitted pulse shape obtained by propagating an impulse through realizations of the synthetic medium. The 20 dotted lines correspond to 20 different realizations of the medium, all with the same length. Note that the travel time to this fixed depth is random.

In Figure 2 we show the same pulses, but now plot them relative to the first arrival time of each pulse at the given depth. When we center the pulses in this way it becomes clear that the apparent diffusion or broadening of the pulse caused by the random medium fluctuations is deterministic and independent of the particular realization. Recall that the initial pulse profile was extremely thin, namely, a delta function. Note also that the center of the impulse can be delayed relative to the accumulated transit time to the given depth. The delay is on the order of the width of the transmitted pulse. The broadening can be derived analytically based on the statistics of the medium fluctuations. The broadening predicted by the pulse shaping theory is shown by the solid line.

For more examples along the same vein, but when the medium model is derived from

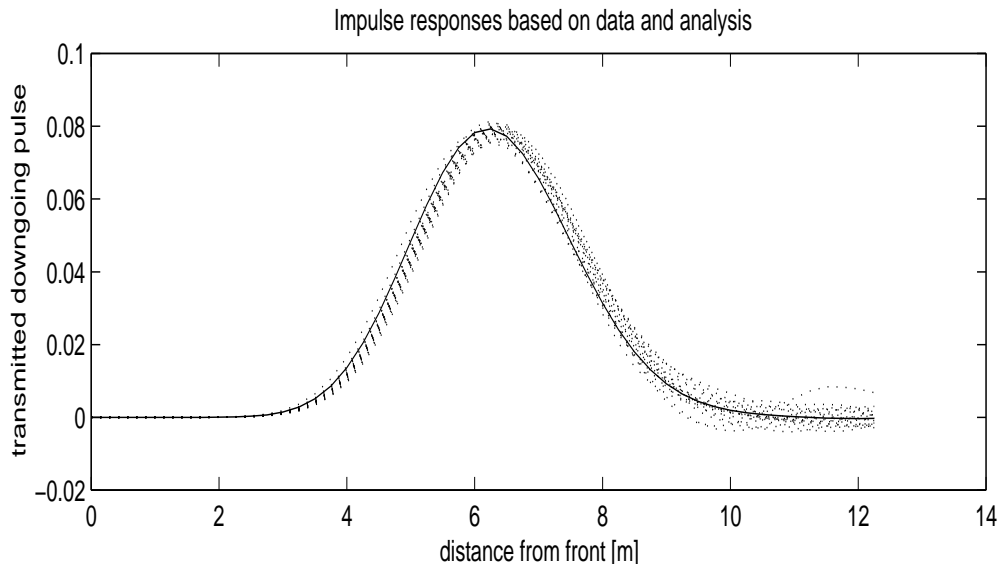


Figure 2: The transmitted pulse shape obtained by propagating an impulse through realizations of the synthetic medium. The 20 dotted lines correspond to 20 different realizations of the medium, and are defined as in Figure 1. However, now they are plotted relative to their first arrival time. Note that the transformation of the pulse shape is deterministic and agrees well with the pulse shaping approximation shown by the solid line.

sonic well logs, see [22].

## 4 The deterministic case

As mentioned above the pulse shaping approximation can be seen as a combination of the geometrical optics approximation with the purely layered pulse shaping theory. Here, we review briefly the geometrical optics approximation associated with acoustic wave propagation from a point source.

A key assumption for the approximation to be valid is that the support of the propagating pulse is short relative to the medium variations, as represented say by the (smooth) variations in the local speed of sound  $c$ . When  $\nu \equiv 0$  in (2) then the local speed of sound

is  $c_1 = \sqrt{K_1/\rho_0}$  and satisfy the assumption about slow variation. A central ingredient of

the geometrical optics approximation are the rays. For a point source these are smooth line segments that emanate radially from the location of the source. The rays are perpendicular to the level curves or surfaces of the phase  $\varphi$  that solves the eiconal equation

$$|\nabla\varphi|^2 = c_1^{-2}. \quad (3)$$

The phase  $\varphi$  gives the *travel time* of the wave front. As the wave propagates in three spatial dimensions it changes its shape due to variations in the local speed of sound and other geometrical effects. This can be described, to leading order, by solving the first transport equation along the geometrical optics rays.

## 5 Main result

When  $\nu \neq 0$  the geometrical optics approximation described in the previous section is not valid in general since the medium varies on a scale that is small relative to the pulse support. For short propagation distances, however, the wave propagation can be described by the geometrical optics approximation relative to the *effective* medium. For long propagation distances the transmitted pulse can be described as the transmitted pulse in the *effective* medium modified in a way that is analogous to the modification for a purely layered medium discussed in Section 3. Below we describe the modification that gives the apparent diffusion of the pulse due to scattering associated with the medium microstructure.

Let  $\mathbf{u}, p$  solve (1)–(3). Furthermore, let  $\varphi$  solve the eiconal equation (3) with a point source at  $(\mathbf{0}, z_s)$ . Note that this corresponds to solving the eiconal equation of the geometrical optics approximation with respect to the *deterministic* part of the medium. This deterministic part actually corresponds to the *effective* medium.

The net effect of the medium fluctuations can be described in the following way. For  $z > 0$ , and with probability 1, we have

$$p(\mathbf{x}, z, \varphi + \chi_\varepsilon + \varepsilon s) \sim [G_f \star \mathcal{N}](s) \quad \text{as } \varepsilon \downarrow 0. \quad (4)$$

The function  $G_f(\mathbf{x}, z, (t - \varphi)/\varepsilon)$  is the transmitted pressure when  $\nu \equiv 0$ , that is, the transmitted pressure in the effective medium which can be characterized by the geometrical optics approximation. The pulse shaping function  $\mathcal{N}$  is, in the simplest case, a centered Gaussian distribution whose square width  $V$  depends on the medium statistics. The convolution above is analogous to the one obtained with the heat kernel, thus justifying the term *apparent diffusion*. The random variable  $\chi_\varepsilon$  is a travel time correction, and gives the time frame in which the pulse shape stabilizes or becomes deterministic.

Let  $\Gamma$  be the part of the geometrical optics ray segment between the source location  $(\mathbf{0}, z_s)$  and the observation point  $(\mathbf{x}, z)$  that is located in the halfspace  $z > 0$ . For the result (4) to be valid we need to assume that this ray segment is smooth and nowhere horizontal. Then

$$V = (l/2) \int_{\Gamma} c_1^{-2} \cos(\theta)^{-1} d\sigma$$

$$\chi_\varepsilon = \int_\Gamma c_1^{-1} \nu / 2 \, d\sigma \quad (5)$$

$$l \equiv \int_0^\infty E[\nu(0)\nu(u)] \, d\sigma,$$

with  $\sigma$  being arc-length along the path  $\Gamma$  and  $\cos(\theta)$  the angle between  $\Gamma$  and the vertical direction. The correlation length  $l$  is a measure of the strength and coherence of the microstructure (microscale medium fluctuations). A key step in deriving the above result is to decompose the wave field in locally up and down propagating components. We describe this decomposition in Appendix A. Additional technical details are given in [19, 21].

The approximation (4) generalizes the one-dimensional pulse shaping approximation. It differs in that the random travel time correction  $\chi_\varepsilon$  and the square width of the modulating pulse,  $V$ , are defined as integrals over the geometrical optics path  $\Gamma$ . In the purely layered horizontal plane-wave case the pulse broadening and random travel time correction are still given by (5) with the path  $\Gamma$  specializing to  $(\mathbf{0}, (0, z))$ .

As in the layered case illustrated in Figures 1 and 2 the approximation (4) modifies the usual high frequency approximation for the effective medium in two important ways.

First, the arrival time of the transmitted pulse is random and given by

$$\tau_\varepsilon = \varphi + \chi_\varepsilon.$$

Recall that  $\varphi$  is the travel time for the geometrical optics approximation of the effective medium. By the central limit theorem it can be shown that  $\chi_\varepsilon$  is a random variable that is approximately normally distributed with variance  $V$ . Thus, the discrepancy between the arrival time in the locally layered medium and the effective medium arrival time is a mean-zero  $O(\varepsilon)$  random quantity and is hence on the scale of the probing pulse. This is clearly observed in Figure 1.

Second, the scattering associated with the fluctuations causes a smearing of the traveling pulse. The asymptotic characterization of this phenomenon is through a convolution with the Gaussian pulse  $\mathcal{N}$ . The convolution is on the scale of the probing pulse, and hence interacts strongly with its shape. The width of the Gaussian pulse is defined in terms of moments of medium parameters along the path  $\Gamma$  *only*, and does not depend on the particular realization. The pulse shaping, though only visible after a long traveling distance, is a *local* phenomenon. The random modulation of the medium parameters, on the finest scale of the model, causes energy to be scattered over to a ‘locally up-propagating’ wave mode, but this energy is quickly scattered back again due to the fluctuations. Hence, only a small amount of energy is carried by the up-propagating wave mode but it is important because the continuous random channeling of energy gradually delays the pulse relative to the first arrival and causes its shape to diffuse and approach a Gaussian. If there is a lot of structure in the fluctuations, that is, strong correlations, then  $l$  will be relatively large. Coherence and strong variability in the random medium modulation means that the random scattering is associated with a stronger smearing of the pulse. Observe that



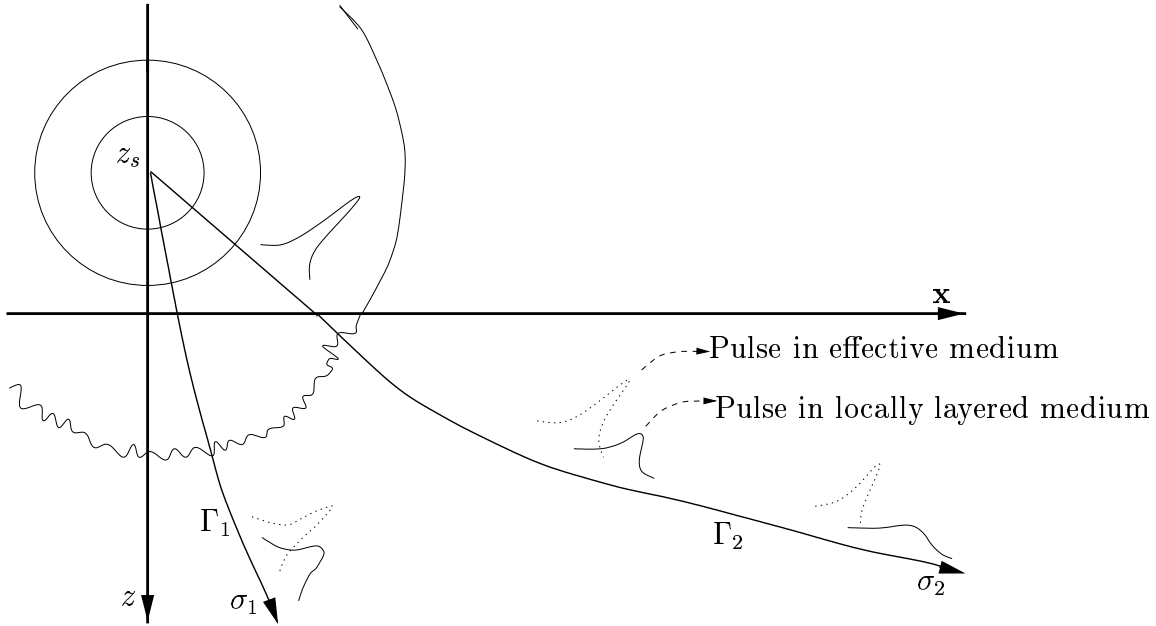


Figure 3: The figure illustrates pulse shaping in a locally layered medium. We plot the pulse shapes as it evolves along two different geometrical optics ray paths. The dotted lines correspond to the pulse shapes in the effective medium. The pulse shapes in the locally layered medium are given by the solid lines. The blurring or smearing of the pulse shapes is due to microscale scattering and is a *deterministic* effect. The travel time of the pulse is corrected by a mean zero *random* variable.

the ‘effective’ correlation length is  $l/\cos(\theta)$ . If the pulse propagates with a shallow angle relative to the layering it ‘sees’ a medium with stronger coherence.

Figure 3 illustrates the above results. The paths  $\Gamma_i$  are geometric optics ray paths associated with a point source at  $(\mathbf{0}, z_s)$  and  $\sigma_i$  the arc-length parameters along these rays. For a set of travel times we plot the traveling pulse in the deterministic or effective medium by the dotted lines. To leading order the evolution of the shapes along the rays is described by the first order transport equations of the geometric optics approximation. The solid lines illustrate the corresponding pulse shapes in the locally layered medium. They are blurred somewhat due to scattering associated with the microscale medium fluctuations. Moreover, the travel time along the ray is corrected by a mean zero random variable. The diffusion depends only on the statistics of the medium fluctuations, whereas the travel time correction depends on the detailed structure of the medium fluctuations along the geometric optics ray path.

## 6 Pulse shaping for shallow water waves

We consider gravity driven surface waves, propagating in shallow channels, in a regime where the fluid is considered to be inviscid, incompressible and the flow is irrotational. Two water wave models in disordered media have been studied. The first is the linear, one-dimensional, potential theory [14, 17]. The second is a nonlinear, three-dimensional, shallow water model [15, 16].

For the potential theory model [23] the following characteristic scales are introduced: the typical depth  $h_0$ , typical wavelength  $\lambda$ , typical amplitude  $a$  of the free surface elevation  $\eta(x, t)$ , horizontal length scale  $l_b$  of the bottom irregularities and  $L$  the total length of the rough region. When using dimensionless variables the following dimensionless parameters appear:  $\alpha = a/h_0$  which controls the strength of the nonlinearity,  $\beta = h_0^2/\lambda^2$  which controls dispersion and  $\gamma = l_b/\lambda$  which controls how rapidly the bottom irregularities vary. The acceleration due to gravity is denoted by  $g$  and the reference shallow water speed

is  $c_0 = (gh_0)^{1/2}$ . Regimes of interest can be identified by expressing the dimensionless parameters in terms of a small parameter  $\varepsilon > 0$  [23].

The problem studied in Nachbin & Papanicolaou [17] is linear ( $\alpha = 0$ ). In order to formulate the reflection-transmission problem a system of stochastic differential equations is derived for the amplitudes of the propagating and evanescent modes, obtained from the eigenfunction decomposition of the time-harmonic velocity potential. The solution to these equations is characterized asymptotically as a diffusion process through the application of a limit theorem for stochastic differential equations. This allows the characterization of the expected value of the transmission or reflection coefficient. Details of the stochastic theory can be found in Asch et al. [1] and references therein.

In this paper we focus on the shallow water equations due to its analogy with the acoustic model, as shown below. The starting point are the Navier–Stokes equations describing constant density, free surface flows of an incompressible fluid. The conservation of momentum equations are

$$u_t + uu_x + vv_y + ww_z = -p_x + \mu(u_{xx} + u_{yy}) + \nu u_{zz} \quad (6)$$

$$v_t + uv_x + vv_y + ww_z = -p_y + \mu(v_{xx} + v_{yy}) + \nu v_{zz} \quad (7)$$

$$w_t + uw_x + vw_y + ww_z = -p_z + \mu(w_{xx} + w_{yy}) + \nu w_{zz} - g. \quad (8)$$

The conservation of mass equation is

$$u_x + v_y + w_z = 0. \quad (9)$$

The horizontal  $x$  and  $y$  velocity components are  $u(x, y, z, t)$ ,  $v(x, y, z, t)$  and the  $z$ -vertical component is  $w(x, y, z, t)$ . Time is denoted by  $t$ , the normalized pressure by  $p(x, y, z, t)$  (i.e. normalized by the constant density) and the horizontal and vertical viscosity coefficients by  $\mu$  and  $\nu$ , respectively.

Integrating the continuity equation (9) over the depth (from the bottom topography  $z = -h(x, y)$  up to the free surface  $z = \eta(x, y, t)$ ) we obtain the following free surface condition in conservative form:

$$\eta_t + \left[ \int_{-h}^{\eta} u dz \right]_x + \left[ \int_{-h}^{\eta} v dz \right]_y = 0. \quad (10)$$

This calculation is exact and is obtained by applying the kinematic condition along the free surface and the impermeability condition along the bottom [6].

A shallow water model is derived by adopting the hydrostatic pressure approximation

$$p(x, y, z, t) \approx p_a(x, y, t) + g[\eta(x, y, t) - z].$$

Without loss of generality, the atmospheric pressure  $p_a$  is assumed to be zero. The hydrostatic approximation is commonly used in shallow water ocean, or atmospheric, models. The vertical convection and diffusion terms are neglected, and the final form for the system of partial differential equations to be solved is given by

$$u_t + uu_x + vv_y + ww_z = -g\eta_x + \mu(u_{xx} + u_{yy}) + \nu u_{zz} \quad (11)$$

$$v_t + uv_x + vv_y + ww_z = -g\eta_y + \mu(v_{xx} + v_{yy}) + \nu v_{zz} \quad (12)$$

$$\eta_t + \left[ \int_{-h}^{\eta} u dz \right]_x + \left[ \int_{-h}^{\eta} v dz \right]_y = 0. \quad (13)$$

The vertical velocity component  $w$  is calculated from the conservation of mass equation. We will refer to the system above as the hydrostatic Navier–Stokes model (HNS model). Further conditions can be incorporated, such as for the tangential boundary stress along the free surface and along the sediment–water interface. We omit these conditions since they are not going to be taken into account in our experiments.

A simplification takes place when we vertically-average over the water body: the model reduces to the shallow water equations

$$U_t + UU_x + VU_y = -g\eta_x + \mu(U_{xx} + U_{yy})$$

$$V_t + UV_x + VV_y = -g\eta_y + \mu(V_{xx} + V_{yy})$$

$$\eta_t + [HU]_x + [HV]_y = 0.$$

where the vertical averages are defined as

$$U(x, y, t) = \frac{1}{H} \int_{-h}^{\eta} u \, dz, \quad V(x, y, t) = \frac{1}{H} \int_{-h}^{\eta} v \, dz$$

and  $H(x, y, t) = \eta(x, y, t) + h(x, y)$ . Linearizing about the undisturbed state, and switching off the effect of viscosity, we obtain the linear shallow water model which can be written in the form

$$\vec{\Psi}_t + (gh)\nabla\eta = 0 \tag{14}$$

$$\eta_t + \nabla \cdot \vec{\Psi} = 0, \tag{15}$$

where the vector discharge function, per unit width, is given by  $\vec{\Psi} = [Uh, Vh]^T$ . The analogy with the linear acoustic model

$$\rho\vec{u}_t + \nabla p = 0 \tag{16}$$

$$\frac{1}{K_\varepsilon(x, z)} p_t + \nabla \cdot \vec{u} = 0 \tag{17}$$

is easily established. The variable shallow water propagation speed is given by  $c_1(x, y) =$

$(gh_1(x, y))^{1/2}$ , where  $h(x, y) = h_1(x, y)(1 + n(x, y))$ . The slowly varying background topography is denoted by  $h_1(x, y)$  and the rapidly varying, locally layered, features by  $n(x, y)$ . The former is called the *macrostructure* of the topography, while the latter the *microstructure*. Recall that for acoustic waves the speed of sound is given by  $c_1(\mathbf{x}, z) =$

$(K_1(\mathbf{x}, z)/\rho)^{1/2}$ .

## 6.1 Interaction with the macrostructure of the topography

To apply ray theory we consider only the *macrostructure* of the topography since it is slowly varying with respect to the pulse scale. This is the deterministic case presented in section 4. Let a generic point be denoted by  $\mathbf{X} \equiv (x, y)$  and suppose that the wave elevation can be written as

$$\eta(\mathbf{X}, t; \mathbf{X}_0) = a(\mathbf{X}; \mathbf{X}_0) \text{P} \left( \frac{t - \tau(\mathbf{X}; \mathbf{X}_0)}{\varepsilon} \right).$$

The notation is such that the initial position of the pulse is  $\mathbf{X}_0$ , its amplitude is given by  $a$  and the phase (or travel time) denoted by  $\tau$ . The pulse profile is denoted by  $P$ . We substitute this ansatz into the shallow water equations. To leading order we get the eiconal equation

$$|\nabla\tau|^2 = c_1^{-2}.$$

Let a ray (characteristic curve) be denoted by  $\mathbf{X}(\sigma)$  and the front propagation direction by  $\mathbf{N} = (n_1, n_2) \equiv \nabla\tau(\sigma)$ . Using the method of characteristics we get Hamilton's equations

$$\frac{d\mathbf{X}}{dt} = \nabla_{\mathbf{N}}\mathcal{H}(\mathbf{X}, \mathbf{N})$$

$$\frac{d\mathbf{N}}{dt} = \nabla_{\mathbf{X}}\mathcal{H}(\mathbf{X}, \mathbf{N}),$$

where  $\mathcal{H}(\mathbf{X}, \mathbf{N}) = 0.5 c_1^2 |\mathbf{N}|^2$ . Subscript variables indicate partial differentiation. Applying to the shallow water model we have

$$\begin{cases} dx/dt = g n_1 h_1(x, y) \\ dy/dt = g n_2 h_1(x, y) \\ dn_1/dt = -0.5 [\ln(h_1(x, y))]_x \\ dn_2/dt = -0.5 [\ln(h_1(x, y))]_y \end{cases} \quad (18)$$

The initial conditions are the initial position of the pulse ( $\mathbf{X}(0) = \mathbf{X}_0$ ) and the initial direction ( $\mathbf{N} = (n_1(0), n_2(0))$ ) for the ray tracing. A ray segment (i.e. path  $\Gamma$ ) is obtained by solving the above system of ordinary differential equations. The initial conditions are the starting point of the ray segment and its initial direction.

## 6.2 Interaction with the microstructure of the topography

We now consider the effect of the fine features of the topography, namely, the locally layered irregularities which are rapidly varying with respect to the pulse scale. The result is analogous to that of acoustic waves (c.f. section 5). Namely we have the apparent diffusion of water waves is expressed by equation (4), with the pressure  $p(\mathbf{x}, z, t)$  replaced by the water elevation  $\eta(x, y, t)$ . The pulse shaping function is also a Gaussian. The schematic description for the pulse propagation is similar to that presented in figure 3, with  $z$  replaced by  $y$ . In other words, for acoustic waves this figure represents a side view of the earth's crust. For water waves it represents a top view of the water body.

## 7 Numerical model

The 3D equations (11–13) are considered in the inviscid regime. They are discretized by an implicit, semi–Lagrangian technique which accomplishes the objective that the stability of the scheme does not depend on the celerity. Based on a linear stability analysis Casulli & Cheng [6] derived a scheme which treats implicitly the hydrostatic pressure gradient term and the velocity terms in the free surface. This method is actually called a semi–implicit scheme because, in the full model, the vertical diffusion term is discretized implicitly while the horizontal diffusion discretization is kept explicit.

The spatial grid consists of rectangular cells, centered at  $(x_i, y_j, z_k)$ , of length  $\Delta x$ ,  $\Delta y$  and height  $\Delta z_{ijk}^n$ . This height is interpreted as the thickness of the  $k$ -th layer of the 3D

grid. Because of the presence of the topography and free surface, this thickness can vary in space and time (indicated by the superscript  $n$ ). The convection terms are treated in a Lagrangian form, through the discretization of the material derivative  $(D/Dt)_{ijk}^n$ . A fixed

staggered grid is defined on the horizontal planes, at the interface between vertical layers. The numerical transport is performed in an Eulerian–Lagrangian manner, relying therefore on the interpolation of the respective grid point–values at the backward–characteristic points of departure. Only one layer was used in the experiments presented below. Details are given in Casulli & Cheng [6] and the references within.

### 7.1 Numerical experiments

We performed experiments to observe pulse propagation over different types of topographies. To normalize the wave celerity we change the acceleration due to gravity so that the reference shallow water speed is always equal to one:  $(gh_0) = 1$  or  $g = 1/h_0$ . The implicit scheme constant is taken to be  $\theta = 0.5$  (Crank–Nicolson). This value minimizes the numerical dissipation. Several validation experiments were performed in Nachbin [15] and Nachbin & Casulli [16]. The experiments revealed that when the parameter  $\alpha = 0.001$  the waves propagate in the linear regime, whereas for  $\alpha = 0.1$  the regime is nonlinear and the waves break into bores.

We synthesize a topography with ingredients geared towards observing features of the theory. The macroscopic variations are such that the wave will have contrasting shallow water speeds over different regions. The reference speed is still equal to one. To achieve this goal we create a topography profile such that the macroscopic depth variation is given by

$$h_1(x, y) = h_1(r, \theta) = h_{00} - a_r r^3 \cos(3\theta),$$

with the constraint

$$h_{min} \leq h_1(x, y) \leq h_{max}.$$

In figure 4 we have a topography where we used  $h_{min} = 100$ ,  $h_{max} = h_0 = 1000$ , depth at the origin  $h_{00} = 500$  and scale factor  $a_r = 500$ . Note that the topography has three

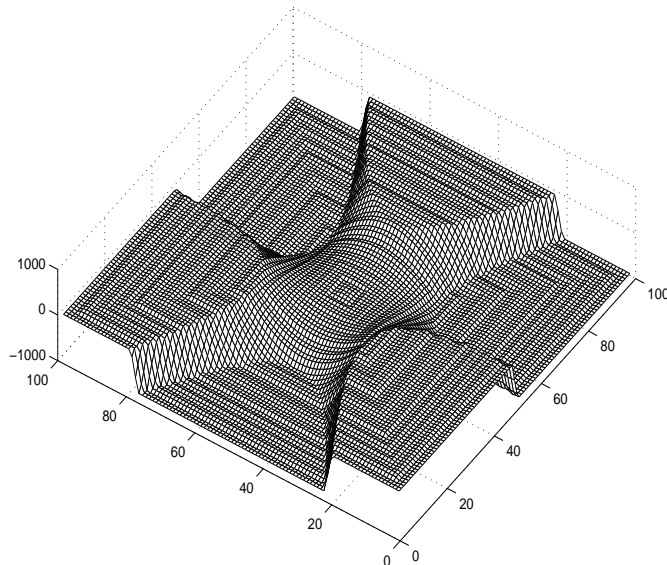


Figure 4: Slowly varying topography with a locally layered microstructure.

flat, mesa-like, shallow parts. Also it has three gorges (narrow passages) in between the mesas.

The initial wave profile is an abandoned axisymmetric Gaussian mound of water. It is abandoned at the center where we see a small square. Note that we have a sequence of centered squares, each indicating a microscopic ridge (layer) with a random height. The heights are uniformly distributed in  $[-30, 30]$ . This is our disordered microstructure. Hence we have a locally layered topography.

We present the results for three different experiments. First we consider a flat topography. As expected, the wave propagates in the radial direction as shown in Figure 5(A). We use the same grid that is necessary for the topography with the microstructure: 1000 by 1000 grid points, with  $\Delta x = \Delta y = 0.01$  and  $\Delta t = 0.0025$ . We use one layer in the vertical direction. Since we are in the shallow water regime there is no need for a finer vertical discretization. In the presence of the topography, a run with 2000 time steps takes approximately 13 hours on a SGI Octane.

In the second experiment we consider only the macroscopic variations of the topography. We are in the ray theory regime. The result is presented in Figure 5(B). We can clearly see how the anular wave bends according to the depth variations. Note that in the deeper regions the wave moves faster and becomes wider with a smaller amplitude. On the other hand, over shallow regions the wave moves slower and peaks, due to mass conservation. We have chosen an amplitude/depth ratio so that the wave does not break. Recall that this linear-experiment is performed with a nonlinear code. The linear regime is obtained by an appropriate choice of scaling parameters.

Finally we consider the full, locally layered topography. The wave profile is roughly the same as in Figure 5(B). We do not present it here due to space constraint. It is important

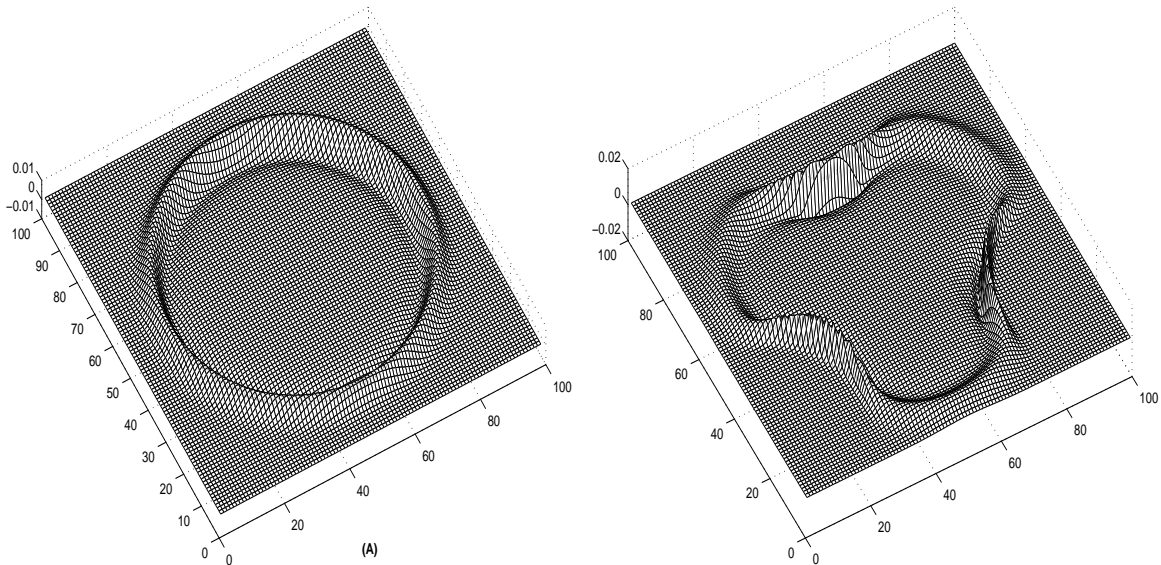


Figure 5: **(A)**: Outgoing wave over a flat bottom. **(B)**: Outgoing wave over the slowly varying topography (i.e. without the microstructure).

to emphasize that the water body used is not large enough for apparent diffusion to be fully developed. In the near future we will perform experiments with a larger grid and longer propagation distances. But there is some indication of the wave interaction with the microstructure. In Figure 6(A) we present a contour plot contrasting the two cases above: topography with a microstructure (dashed line) and without (solid line). Note that they are very similar over the deeper part but differ over the shallow regions. In the shallow regions the peaked wave is delayed by the microstructure. The delay is in the same direction as the rays. The separation between the contour lines is basically the same, indicating that pulse broadening is not yet taking place. For this to happen we need longer propagation distances, as we know from the theory. In Figure 6(B) we have the wave profiles along the diagonal our grid. As a matter of fact, there is a very mild indication of apparent attenuation. As mentioned above, we are investigating this issue in more detail.

## 8 Acknowledgements

We are grateful to George Papanicolaou (Stanford University, USA) for establishing the contact between us and for providing support while we attended, and initiated our collaboration at the 1998 Mathematical Geophysics Summer School, held at Stanford University.

A. Nachbin would like to thank Vincenzo Casulli (Università di Trento, Italy) for the copy of his 3D hydrostatic Navier–Stokes code (TRIM3D) and Greg Kriegsmann (New



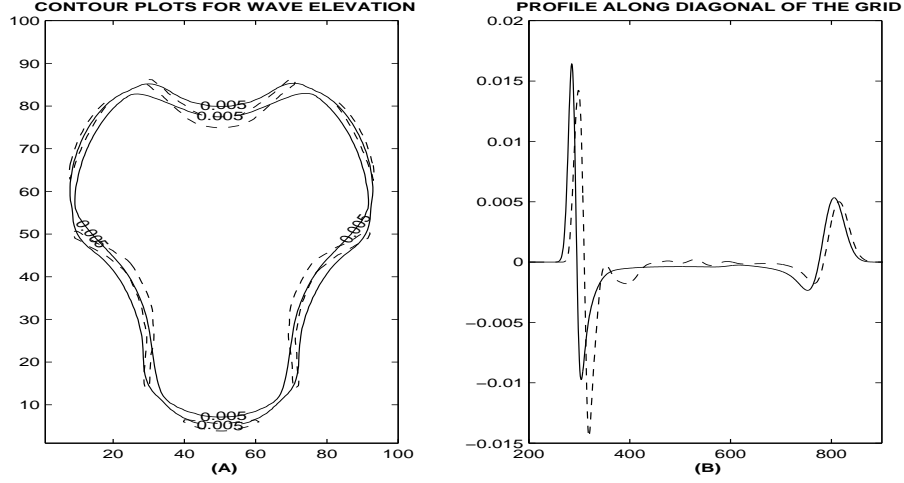


Figure 6: **(A)**: Contour plots for the wave elevation. The dashed line represents the experiment with the locally layered topography. The solid line represents the variable topography without the microstructure. **(B)**: Water elevation profile plotted along the grid's diagonal ( $\eta_{ii}$ ).

Jersey Institute of Technology, USA) for his hospitality and support during a visit which played an important role in getting this project started.

A. Nachbin's work was supported in part by: CNPq under Grant 300368/96-8; CNPq under Grant CNPq/NSF 910029/95-4; and NEC/CEMAT under Grant DMS 2.419/98-00.

K. Sølna's work was supported in part by the Research Council of Norway.

## A Decomposition of wave field

In order to derive the result (4) we decompose the pulse approximately into a superposition of up and down going waves, which is analogous to what is done in the *layered* case with plane waves :

$$\begin{aligned}
 p(\mathbf{x}, z, t) = & \int \int \int [A(\mathbf{x}, z, \omega, \boldsymbol{\kappa}) e^{i\omega S^+(\mathbf{x}, z, \boldsymbol{\kappa})/\varepsilon} \\
 & + B(\mathbf{x}, z, \omega, \boldsymbol{\kappa}) e^{i\omega S^-(\mathbf{x}, z, \boldsymbol{\kappa})/\varepsilon}] e^{i\omega t/\varepsilon} d\boldsymbol{\kappa} dt.
 \end{aligned} \tag{19}$$

In the layered case the phases are  $S^\pm = \boldsymbol{\kappa} \cdot \mathbf{x} \pm \tau(z)$  where  $\tau(z) = \int_0^z \sqrt{\rho_0/K_1(z)} dz$  is the

travel time and  $A = A(\boldsymbol{\kappa}, z, \omega)$ ,  $B = B(\boldsymbol{\kappa}, z, \omega)$  the down and up going wave amplitudes. This amounts to a Fourier representation relative to horizontal space variables. In the *locally layered* case we cannot take the horizontal Fourier transforms. Now the phases  $S^\pm$  solve the eiconal equation

$$(\nabla S^\pm)^2 = \frac{\rho_0}{K_1(\mathbf{x}, z)} \equiv c_1^{-2}(\mathbf{x}, z) \quad (20)$$

associated with the deterministic effective medium parameters. In the purely layered case these are plane wave phases. The appropriate coupling between the amplitudes  $A$  and  $B$  of the locally up and down going wave fields is dictated by the microscale structure. This leads to the generalized transport equations

$$2\nabla S^+ \cdot \nabla A + \Delta S^+ A - i(\omega/\varepsilon)c_1^{-2} \nu \{A + \tilde{B} e^{i\omega\Phi_1/\varepsilon}\} = R^+ \quad (21)$$

$$2\nabla S^- \cdot \nabla B + \Delta S^- B - i(\omega/\varepsilon)c_1^{-2} \nu \{B + \tilde{A} e^{i\omega\Phi_2/\varepsilon}\} = R^-.$$

Here  $R^\pm$  are lower order terms,  $\Phi_i$  are phase functions and  $\tilde{A}$ ,  $\tilde{B}$  are the wave amplitudes  $A$ ,  $B$  at a different  $\boldsymbol{\kappa}$  argument. We have thus reduced the original problem to the analysis of these transport equations, which are complicated stochastic equations. They contain, however, the simplifications that come from the geometrical acoustics approximation in the locally layered medium and this enables us to push through the analysis that leads to the approximation (4). When the random fluctuation  $\nu \equiv 0$ , the transport equations decouple into the usual ones of geometrical acoustics for the local wave amplitudes  $A$  and  $B$ . In the layered case,  $R^\pm \equiv 0$  and equation (21) simplify to the stochastic ordinary differential equations (2.27) in [1].

## References

- [1] M. Ash, W. Kohler, G. C. Papanicolaou, M. Postel and B. White, *Frequency content of randomly scattered signals*, SIAM Review, V 33, 519-625, (1991).
- [2] Burridge R., H. -W. Chang and M. V. De Hoop, *The pseudo-primary field due to a point source in a finely layered medium*, Geophysical Journal International, V 104, 489-506, (1991).
- [3] Burridge R., H. -W. Chang and M. V. de Hoop, *Wave propagation with tunneling in a highly discontinuous medium*, Wave Motion, V 13, 307-327, (1991).

- [4] Burridge R. and P. Lewicki and G. C. Papanicolaou, *Pulse stabilization in a strongly heterogeneous layered medium*, Wave Motion, V 20, 177-195, (1994).
- [5] Burridge R., G. C. Papanicolaou and B. White, *One dimensional wave propagation in a highly discontinuous medium*, Wave Motion, V 10, 19-44, (1988).
- [6] Casulli, V., and Cheng, R.T., *Semi-implicit finite difference methods for three-dimensional shallow water flow*, Int. J. Num. Meth. Fluids, vol. 15, pp. 629-648, (1992).
- [7] Clouet J. F. and J. P. Fouque, *Spreading of a pulse travelling in random media.*, Annals of Applied Probability, V 4, 1083-1097, (1994).
- [8] R. Dashen, W. H. Munk, K. M. Watson and F. Zachariasen, *Sound transmission through a fluctuating ocean*, Editor S. Flatte, Cambridge University Press, 1979.
- [9] Kim M and Y. F. Hwang, *An analysis of wave propagation in coarsely laminated composite plates*, J.Acoust. Soc. Am., V 100, 1981-1991, (1996).
- [10] Kim K. Y., W. Zou and W. Sachse, *Wave propagation in a wavy fiber-epoxy composite material: Theory and experiment*, J. Acous. Soc. Am., V 103, 2296-2301, (1998).
- [11] Kohler W. and G. Papanicolaou, *Asymptotic theory of mixing stochastic ordinary differential equations.*, Comm. Pure Appl. Math., V 27, 614-668, (1974).
- [12] Lewicki P., *Long time evolution of wavefronts in random media*, SIAM J. Appl. Math., V 54, 907-934, (1994).
- [13] Lewicki P., R. Burridge and M. V. de Hoop, *Beyond Effective Medium Theory: Pulse Stabilization for Multimode Wave Propagation in High Contrast Layered Media.*, SIAM Journal on Applied Math., V 56, 256-276, (1996).
- [14] Nachbin A., *The localization length of randomly scattered water waves*, J. Fluid Mech., V 296, 353-372, (1995).
- [15] Nachbin A., *The effective behaviour of linear and nonlinear waves in irregular channels*, submitted for publication, (1999).
- [16] Nachbin A. and V. Casulli, *Water waves: linear potential theory results validated with a hydrostatic Navier-Stokes model*, In: Mathematical and Numerical Aspects of wave Propagation, Editor J. A. DeSanto, SIAM, (1998).
- [17] Nachbin A. and G. Papanicolaou, *Water waves in shallow channels of rapidly varying depth*, J. Fluid Mech., V 241, 311-332, (1992).
- [18] O'Doherty R. F. and N. A. Anstey, *Reflections on amplitudes*, Geophysical Prospecting, V 19, 430-458, (1971).
- [19] Papanicolaou G. and K. Sølna, *Ray theory for a locally layered random medium*, submitted to Waves in Random Media, (1998).

- [20] Shapiro S. A., P. Hubral and B. Ursin, *Reflectivity/transmissivity for 1-D inhomogeneous random elastic media: dynamic-equivalent-medium approach.*, Geophysical Journal International, V 126, 184-196, (1996).
- [21] Sølna K., *Stable spreading of acoustic pulses due to laminated microstructure*, Thesis, Stanford University, (1997).
- [22] Sølna K., *Estimation of pulse shaping for well logs*, submitted to Geophysics, (1998).
- [23] Whitham G. B. *Linear and nonlinear waves*, John Wiley, (1974).